STM JOURNALS

Journal of
Polymer & Composites

ISSN: 2321-2810 (Online)
ISSN: 2321-8525 (Print)
Volume 13, Issue 2, 2025
DOI (Journal): 10.37591/JoPC

https://journals.stmjournals.com/JOPC/

Review JoPC

Green Synthesis and Evaluation of Electronic and Optical Properties of CdS/CdTe Quantum Dots

Ravindar Adla[1], Veeraswamy Maragani[2], Suresh Kumar Danikonda[3], Bikshamaiah Nampally[4], Madhuri Dumpala[5], Madhukar Katakam[6,*]

Abstract

The CdS/CdTe quantum dots (QDs), with altered concentrations of CdS, were synthesized using straightforward precursors through an environmentally friendly green method. The synthesized quantum dots were characterization by UV–visible absorption spectroscopy, Photoluminescence (PL), and Fourier Transform Infrared Spectroscopy (FTIR) to understand their electronic and structural properties. The average particle size is nearly consistent with the values derived from Brus's formula. The UV–visible spectra show a blueshift compared with pure sample, this could be attributed as quantum size effect on electron and hole. The band gap energy ranges from 2.71 eV to 2.32 eV indicating tunable optical properties. Band gap energy decreases as the size of quantum dots increasing. The band gap energy of system was determined from absorption data, using a Tauc plot, yielding a value of 2.71 eV. The FTIR showed a significant vibrational peak near 732 cm^{-1}, indicating the presence of the Te-O and carbonyl group C=O. The estimated band gap of CdS/CdTe based quantum dots, determined through Tauc plot analysis, is 2.59 eV. The PL emission peak range from 500-650 nm show size dependent of optical properties. The PL spectra show a strong and narrow emission peak, indicating high quantum efficiency. The preset work is aimed to enhance the characteristics of CdTe/CdS properties suitable for energy conversion and to further stimulate interest, as the emission of CdS/CdTe QDs exhibits peaks positioned at 608 nm, attributed to the presence of cadmium ions vacancies align qualitatively.

***Author for Correspondence**
Madhukar Katakam
E-mail: mkatakam@osmania.ac.in

[1]Research Scholar, Department of Physics, Polymer Nanocomposites and Functional Materials Laboratory, University College of Science, Osmania University, Hyderabad, Telangana, India
[2]Research Scholar, Department of Physics, Polymer Nanocomposites and Functional Materials Laboratory, University College of Science, Osmania University, Hyderabad, Telangana, India
[3]Assistant Professor, Department of Physics, University P G College, Satavahana University, Godavarikhani, Telangana, India
[4]Assistant Professor, Department of Physics, University College of Science, Mahatma Gandhi University, Nalgonda, Telangana, India
[5]Assistant Professor, Department of Physics, Polymer Nanocomposites and Functional Materials Laboratory, University College of Science, Osmania University, Hyderabad, Telangana, India
[6]Professor, Department of Physics, Polymer Nanocomposites and Functional Materials Laboratory, University College of Science, Osmania University, Hyderabad, Telangana, India

Received Date: January 06, 2025
Accepted Date: February 17, 2025
Published Date: March 25, 2025

Citation: Ravindar Adla, Veeraswamy Maragani, Suresh Kumar Danikonda, Bikshamaiah Nampally, Madhuri Dumpala, Madhukar Katakam. Green Synthesis and Evaluation of Electronic and Optical Properties of CdS/CdTe Quantum Dots. Journal of Polymer & Composites. 2025; 13(2): 185–194p.

Keywords: CdS/CdTe, Quantum dots, UV-Vis, Photoluminescence, FTIR, band gap energy

INTRODUCTION

The Semiconductor nanostructures represent a highly studied category of advanced materials, owing to their significance in fundamental research and their extensive array of technological applications. The characteristics of semiconductors at the nanometer scale are significantly influenced by their dimensions, as there is a high in the energy gap compared to bare materials, and their elevated exact surface area leads to enhanced chemical reacted responsiveness. The different semiconductor quantum dots (QDs) display two unique physical and chemical properties. Dimensions approach the Bohr exciton radius, with the quantum confinements effects resulting in adjustable optical characteristics [1 ,2]. The

blueshift observed in photoluminescence and in optical absorption of nano-sized indicates semiconductors illustrates this effect clearly. The influence of quantum confinements on the optical characteristics of QDs is a topic of significant concentration and underpins their various application in imaging and optoelectronics devices [3]. The CdS is classified as an II–VI group semiconducting material and its nanoparticles used attracted significant attention [4]. The CdS using characterized by with its optical direct band gap energy of 2.54 eV, in show found extensive applications in various domains including electrical devices and related insulators of materials, photo electrocatalysts, and optoelectronic devices, in arrears to its nonlinear metal optical properties of materials. The CdS exhibits the distinct zinc blend crystal structures cubic, the different stages of phase. The CdS various nanocrystalline of phase identified hexagonal [5–7]. The growth of base CdS nanoparticles can be achieved through various techniques [8].

This communication outlines the synthesis of nanocrystalline CdS using green technique. The prepared thin films undergo several investigations to assess their structural, optical, and electrical properties. Consequently, applications utilizing these materials demonstrate significantly higher efficiency in comparison to those that rely on conventional nanomaterials and bulk substances [9,10]. The size of quantum dots in semiconducting nano materials significantly influences their optical properties, including absorbance and transmittance. This, in turn, affects the range of the optical energy gap and makes them suitable for different applications. The CdS/CdTe quantum dots are significant semiconducting crystals, characterized by a direct energy gap of approximately 2.59 eV. Consequently, CdTe has found extensive application in various fields [11]. The synthesis of colloidal nanomaterials is among the most prevalent technique for the synthesis of quantum dots. The colloid synthesis can be approached through two distinct method, the first involves the use of aqueous solvents, known as aqueous synthesis, while the second utilizes non-aqueous solvents, referred to as organometallic synthesis. Here in this work, a green synthesis is employed for the preparation of CdS/CdTe with different concentrations of CdS, QDs, because it is cost-effective, environmentally friendly (compatible with biological environments, i.e., non-toxic), and allows for straightforward tuning of their energy gap [12–14]. In both preparation processes, surface ligands establish intricate bonds with Cd+ ions through the utilization of either polar hydrocarbon chains or charged groups. The presence of ligands on the surfaces of nanoparticles contributes to their stability against aggregation during adsorption or desorption processes, as they function as insulator between individual nanoparticles.

S. S. Nath et al., synthesized CdS/CdTe QDs using a green sol-gel method. The resulting QDs exhibit excellent optical properties, including high photoluminescence efficiency and tenable emission wavelengths, makes them suitable in optoelectronics and several other applications [15]. CdS/CdTe QDs were synthesised by hydrothermal method by Y. Zhang et al with tunable optical properties, such as controlling size, and shape, which make them promising materials for optoelectronic devices, biomedical imaging, and sensing applications. Cadmium sulfide (CdS) and cadmium telluride (CdTe) QDs are particularly interesting due to their tunable optical properties and high photoluminescence efficiency [16]. Cadmium sulfide (CdS) and cadmium telluride (CdTe) QDs are particularly interesting due to their high photoluminescence efficiency and tunable optical properties. A. K. Singh et al., report a novel microbial synthesis method for CdS/CdTe QDs using Bacillus subtilis, a Gram-positive bacterium. The resulting QDs exhibit high photoluminescence efficiency, tunable emission wavelengths, and improved stability [17].

The CdS/CdTe QDs were synthesized using the *Euphorbia jatrophoa* leaf extract and they exhibited good photoluminescence efficiency and tunable optical properties. Furthermore, this method can be easily scaled up for large-scale production of QDs, making it a promising approach for industrial applications [18]. J. Liu et al. used sol-gel method, successfully, to synthesize CdS/CdTe quantum dots with enhanced optical properties. The resulting quantum dots had a strong emission peak, high quantum yield, and tunable optical properties, making them suitable for various applications, including optoelectronic devices and biomedical imaging. The absorption spectra showed that the particles had a

strong absorption peak. The quantum yield of the CdS/CdTe quantum dots was measured to 30%. The resulting quantum dots were characterized using various techniques [19]. An hydrothermal method was used to synthesize CdS/CdTe QDs by Y. Wang et al. The resulting QDs exhibit high photoluminescence efficiency, tunable emission wavelengths, and improved stability [20]. A. K. Singh et al. used microbial method to synthesise CdS/CdTe quantum dots (QDs) and the results demonstrate the potential of this method for the production of QDs with tailored optical properties [21]. These promising material has various applications, including optoelectronic devices, biomedical imaging, and sensing.
Table 1a summarizes the comparison of the earlier work, based on the different synthesismethods of Cds/CdTe quantum dots along with the present work.

The CdS/CdTe semiconducting quantum dots have attracted significant attention due to their unique optical and electrical properties. Here in this work, the CdS/CdTe QDs were synthesized using leaf extract, a green method, and studies their electronics and optical properties, and the results are highly encouraging. The photoluminescence spectra of the CdS/CdTe quantum dots show a strong emission peak at around 607 nm. This means that they're able to convert light energy into a specific colour.

EXPERIMENTAL TECHNIQUES

Materials and Method

Materials

The Cadmium sulphate ($CdSO_4$) (99.5% from SRL, m.w. 256.50), Tellurium powder (Te) (m.w. 78.96) from Sigma-Aldrich Pvt. Ltd. Methanol (CH_3OH) (m.w. 32.04), Chloroform ($CHCL_3$), Sodium sulphate (Na_2SO_4) of AR grade is from SD Fine Chemicals Ltd., India. Fresh *Moringa oleifera* leaves were gathered from local gardens in Hyderabad, India.

Preparation of Plant Extract

Fresh *Moringa oleifera* (MO) leaves were collected from the local garden near the University College of Science, Osmania University campus, Hyderabad, India. These leaves were thoroughly washed several times with distilled water to remove impurities. After air-drying in the shade for 5 hours, the leaves were finely cut and ground using a micro-grinding machine. About 20 g sample of these ground leaves were mixed with 100 mL of methanol. The mixture was incubated at 70°C for 90 minutes. The resulting solutions were filtered using Whatman No. 1 filter paper, yielding a clear plant extract for further use.

Preparation of CdS and CdTe Quantum Dots

To synthesize CdS and CdTe quantum dots, a solution of 0.25 M $CdSO_4$ in 5 mL of distilled water was prepared and stirred for 20 minutes. Different concentrations of 0.24 M, 0.57 M, and 1.28 M solutions were prepared for further use.

A 1:1 molar ratio of 10 mL of 0.24 M $CdSO_4$ and 0.57 M Tellurium (Te) powder was dissolved in 15 mL of distilled water and stirred for 40 minutes, producing a clear, soluble solutions.

Table 1a. Comparison of the earlier work based on the different synthesis methods of CdS/CdTe quantum dots, with the present work

S.N.	Compound	Synthesis	Size (nm)	Optical properties	Applications	Reference, Year
1	Cd $(NO_3)_2$, TeO_2	Sol-gel	2-5	UV, PL	Optoelectronics	[15], 2012
2	$CdCl_2$, TeO_2	Hydrothermal	5-10	UV, PL	Biomedical imaging	[16], 2011
3	$Cd(NO_3)_2$, TeO_2	Microbial	10-20	UV, PL	Environmental sensing	[17], 2012
4	$Cd(NO3)_2$, TeO_2	Plant-mediated	2-5	UV, PL	Biomedical applications	[18], 2013
5	$Cd(CH_3COO)_2$, TeO_2	Sol-gel	5-10	UV, PL	Optoelectronics	[19], 2012

6	$CdCl_2$, TeO_2	Hydrothermal	10-20	UV, PL	Biomedical imaging	[20], 2013
7	$Cd(NO_3)_2$, TeO_2	Microbial	5-10	UV, PL	Environmental sensing	[21], 2014
8	CdS/CdTe	Green method	3-8	UV, PL	Electrical and optical application	Present work

This was used as a precursor in the synthesis of CdTe nanoparticles. In the first phase, 15 mL of 0.24 M $CdSO_4$ is prepared and combined with 15 mL of CdTe solution [at concentrations of 0.24 M and 0.57 M] and 20 mL of Moringa oleifera leaf extract. In the second phase, 15 mL of 0.14 M Na_2SO_4 was added to the mixture and incubated under similar conditions for an additional 5 days. The resulting solution was centrifuged to isolate nanoparticles. The nanoparticles were then dried in a hot air oven at 90 °C for 3 hrs, producing a dry solid pellet for further characterization studies. The process is shown in Figure 1.

The FTIR analysis of CdS/CdTe

FTIR analysis of the CdS/CdTe quantum dots, synthesized with different CdS concentrations is shown in Figure 2 and peak positions in Table 1b. The FTIR spectra indicate CdS at 621 cm^{-1} the symmetric stretching modes associated with Cd-S are more prominent among the vibrational modes. A significant vibrational peak is detected at about 732 cm^{-1} of indicating the existence of Te-O. T0.5 of 770 cm^{-1} Peaks detected in this range may indicate the existence of secondary phases or contaminants including fluctuations in the stoichiometry of cadmium oxides [22, 23]. At 810 cm^{-1} the vibrations associated with C-C in CdTe quantum dots display remnants from the synthesis deposition processes [24]. The significant peak of S–H vibrations detected in the CdTe spectra indicates the existence of covalent bonding at 978 cm^{-1} the surface of the material. The existence of a peak at 987 cm^{-1} indicates that anharmonic vibrations of Cd-Te bonds may be detected in this region [25,26]. The 1098 cm^{-1} peak in this area often correlate with hydroxyl (OH) groups due to adsorbed water molecules. The T0.5 recorded at 1162 cm^{-1} peak in this area are commonly noted for CdS/CdTe materials, signifying particular surface processes and supplementary functions [27]. The presence of CdS at 1380 cm^{-1} is ascribed to the N-H groups, offering a comparative examination of the FT-IR spectra for CdTe QDs synthesized under different conditions in relation to pure CdS. The synthesis of CdS/CdTe quantum dots.

Photoluminescence spectroscopy of CdS/CdTe

The Photoluminescence spectroscopy serves as a green method for detecting optical alterations through modifications that are evident in the characterization of peak positions and bands. The band emission of PL spectra.

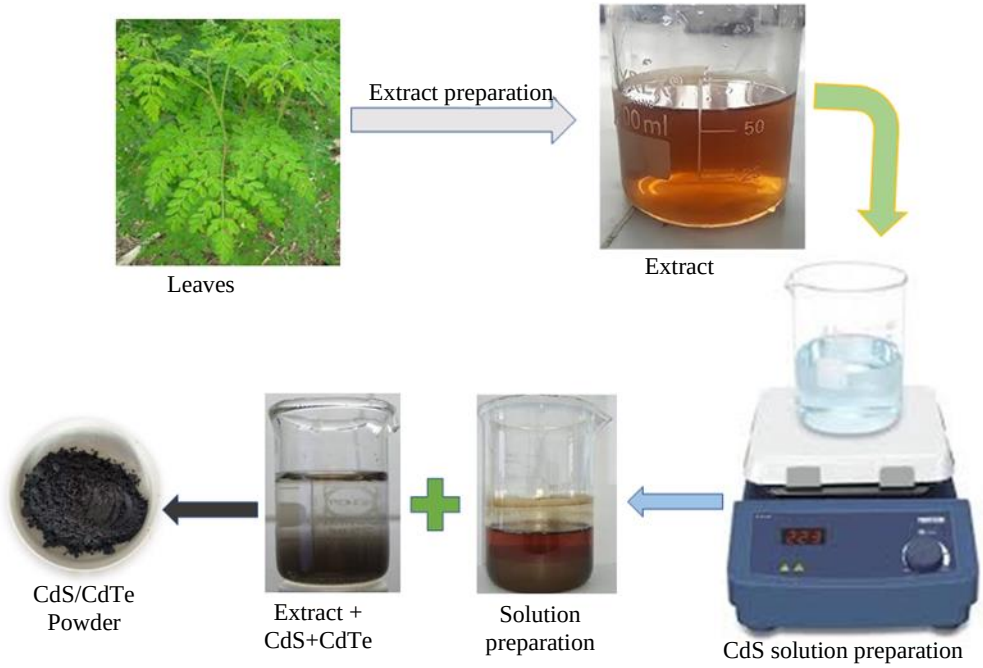

Figure 1. Green method of preparing CdS/CdTe quantum dots.

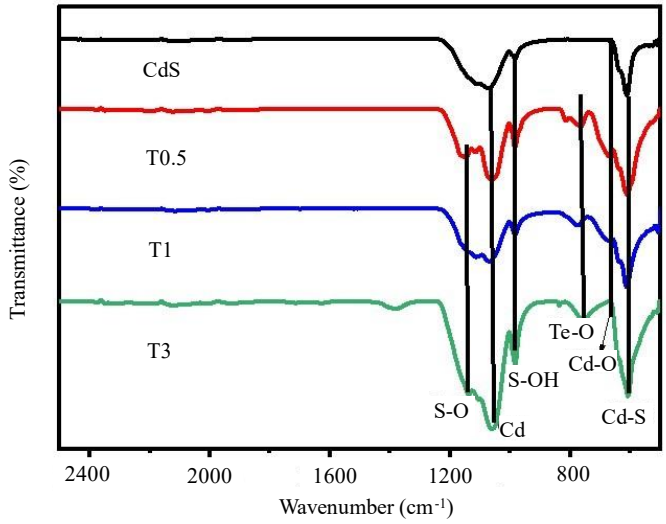

Figure 2. FTIR Spectra of CdS/CdTe with different CdS concentrations.

Table 1b. FTIR peak positions of CdS, T0.5, T1, T3.

Vibrational modes	CdS	T0.5	T1	T3
Cd-S stretching vibration	621	652	676	612
Te-O stretching vibration	-	770	766	-
C-C stretching vibration	-	810	-	826
S-OH stretching vibration	987	980	978	980
C–O Stretching vibration	1098	1054	1074	1067
S-O stretching vibration	-	1162	1144	1149
N-H stretching vibration	-	-	-	1380

Table 2. Photoluminescence λ Max of CdS, T0.5, T1, T3.

S.N.	Sample	E_m [λ max]

1	CdS	608
2	T0.5	605
3	T1	598
4	T3	595

The Figure 3 displays the PL emission spectra of the CdS peak indicating quantum dots at 570 nm revealing peak that correspond to defect emission. lead to the presence of defect states in the forbidden gap, resulting in expected outcomes [28,29]. The cadmium cation vacancies and interstitial sulfur ionic radius function as acceptors. The emissions peak of CdS nanoparticles specifically in different colours indicated have been thoroughly examined [30]. The figure clearly shows the peak associated with band emission and defect emission overlapped. The imperfection emission peaks in CdS quantum dots reveal the photoluminescence spectra exhibit a broadband emissions max ranging from 500 to 650 nm, with a peak around 605 nm, which is associated with the combination of carrier surface positions. Previous investigations on CdS have similar results, this kind of broad emission in the nm scale range [31]. The cause due to the ion's vacancies either cadmium or sulfur dependent upon the presence of the cations. The extensive CdS emanation observed at 608 nm potentially be attributed to cadmium ions vacancies present on the surface. The surface states resulting from Te cation vacancies can function as hole trick positions. Consequently, the extensive T1 emission observed at 598 nm could also be linked to the relaxation of the carrier transitioning from an excitonic state to a surface trap state. The low intensity of T3 band resembling a shoulder at approximately 595 nm is associated with sulfur ion vacancies [32]. The photoluminescence data corroborate the optical absorption findings, indicating a notable enhancement in potential eminence. The Table 2 summaries λ max values.

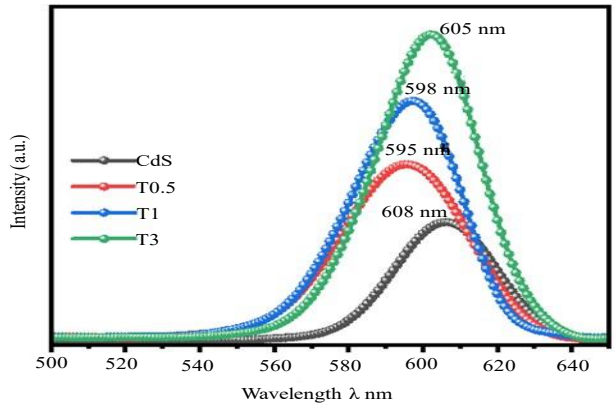

Figure 3. The photoluminescence spectra of CdS/CdTe with different concentrations of CdS.

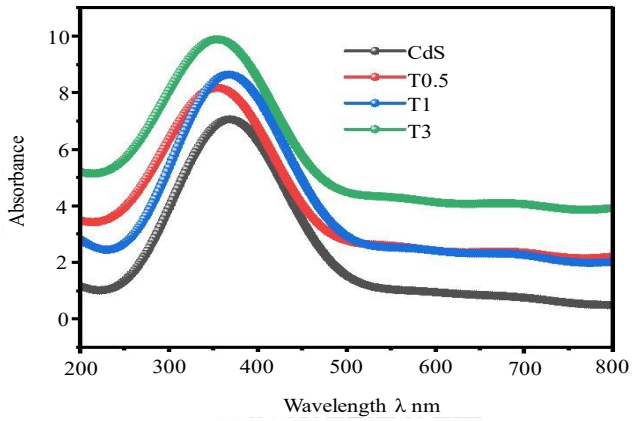

Figure 4. The UV-Vis absorbance spectra of CdS/CdTe with different loadings along with CdS.

UV-Visible and Bandgap Energy of CdS/CdTe

The direct measurement of individual quantum dot sizes is challenging due to the aggregation tendency of nanostructures. Nonetheless, UV-visible absorption spectra and spectra can still facilitate the determination of the average sizes of quantum dots. The UV–visible is an effective method for assessing the characteristics. The wavelength corresponding to maximum exciton absorption diminishes with a reduction in nanoparticle size, due to the quantum confinements of photo-generated electron-holes pairs [33, 34]. The Figure 4 illustrates the UV–visible absorption spectra of the synthesized nanoparticles. The initiation of absorbance peak at around 336 nm is contingent upon nanoparticle size. The quantum size effect causes the absorption peak to shift to shorter wavelengths as particle size decreases compared to bulk materials. The absorption spectra indicate a significant peak in the absorbance of the samples relative to pure CdS, resulting in a high, in the materials band Eg, due to size-induced quantum confinement.

The Table 3 shows the peak positions of samples CdS, T0.5, T1, and T3 and corresponds to the wavelength 354, 325, 329, and 334 nm. Compare to CdS, the other samples showed decreased the peak positions and increased absorbance, with the increased contents of CdS.

Table 3. UV-Visible absorbance peak position of CdS, T0.5, T1, T3 samples.

S.N.	Samples	Wavelength [nm]	Absorbance
1	CdS	354	1.32
2	T0.5	325	2.46
3	T1	329	3.88
4	T3	334	4.63

The direct band gap energy of semiconductors such as CdS, can be determined using the Tauc equation [35].

$$(\alpha h\vartheta)^2 = A[h\vartheta - E_g] \quad (1)$$

Where, A is a constant, hϑ is the photons energy of the input radiation, h is the Planck constants, ν is the photon frequency and E_g of CdS quantum dots.

The optical Eg can be determined from the absorbance by plotting a graph between $(h\vartheta)^2$ verses $h\vartheta$ and thereafter extra peak the linear fit to the energy as shown in Figure 5. The calculated Eg values for the samples CdS, T0.5, T1, and T3 derived from their respective Tauc plot, are approximately 2.71, 2.59, 2.41, and 2.32 eV, respectively, as detailed in Table 4. The size-induced expansion of the Eg can be attributed to strong quantum confinement [36]. The confinement of electron and holes the dimensions of the nanostructures [37, 38]. The relationship between Eg and particle size can be elucidated by the current mass estimate, represented by the following equation.

$$E_g(nano) - E_g(bulk) = \frac{h^2\pi^2}{2r^2}\left[\frac{1}{m_e^*} - \frac{1}{m_h^*}\right] \quad (2)$$

Representing the mass of free electrons. The mean different various of particle size of CdS, with an energy gap (E_g) of 2.71 eV, was computed to be r = 2.1 nm, aligning well with the dimensions [39, 40].

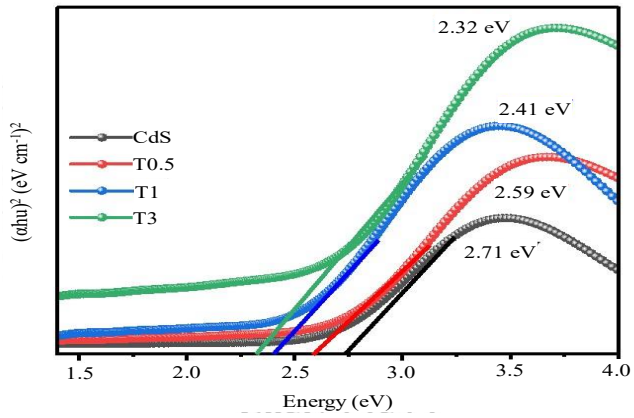

Figure 5. Direct bandgap energy of CdS/CdTe with different concentrations of CdS.

Table 4. Bandgap energy E_g of CdS, T0.5, T1, T3.

S.N.	Samples	E_g[eV]
1	CdS	2.71
2	T0.5	2.59
3	T1	2.41
4	T3	2.32

CONCLUSIONS

The investigation of, green synthesized CdS/CdTe quantum dots with different concentrations of CdS, reveals their exceptional optical characteristics, featuring adjustable ultraviolet (UV) absorption and unique bandgap energies shaped by the quantum confinement effect. The analysis using Fourier-transform infrared spectroscopy (FTIR) provided essential information regarding surface functional groups and chemical bonding, and the photoluminescence (PL) measurements validated the efficient and stable emission properties. The optical band gap measures 2.59 eV, surpassing the bulk value of 2.41 eV, indicating a blueshift as particle size decreases. The photoluminescence emission peaks observed at 608 nm are associated with the existence of cadmium ion vacancies. The FTIR spectrum reveals that C=O and C-O-H stretching vibrations are predominant. The results emphasize the capabilities of CdS/CdTe quantum dots in various applications, including optoelectronics and bioimaging. The improved photophysical properties of these materials make them strong contenders for advanced technologies that demand accurate optical and electronic applications.

REFERENCES

1. Maghouli M, Eshghi H. Studying the effect of deposition time on physical properties of CdTe thin films; Influence of CdTe electrical properties on CdS/CdTe heterojunction rectifying behavior. Optik (Stuttg). 2020 Sep;218:165132.
2. Kudii D, Meriuts A, Khrypunova A, Shelest T, Varvianska V, Zaitsev R. Theoretical Analysis of Optical Properties of CdS/CdTe Film Heterosystems. In: 2020 IEEE 4th International Conference on Intelligent Energy and Power Systems (IEPS). IEEE; 2020. p. 135–9.
3. Ahmed M, Bakry A, Shaaban ER, Dalir H. Structural, electrical, and optical properties of ITO thin films and their influence on performance of CdS/CdTe thin-film solar cells. Journal of Materials Science: Materials in Electronics. 2021 Apr 1;32(8):11107–18.
4. Sofia JR, Wilson KSJ. Investigations on Integration of CdS/CdTe Thin Film Solar Cell with Supercapacitor. Applied Solar Energy. 2024 Apr 26;60(2):215–25.
5. Surucu O, Surucu G, Gasanly NM, Parlak M, Isik M. Exploring Temperature-Dependent bandgap and Urbach energies in CdTe thin films for optoelectronic applications. Mater Lett. 2024 Oct;373:137078.
6. Fadhil EAA, Abdullah MM, Lafta FM. Preparation of N-A Cysteine-capped CdTe/CdS/ZnS core/shell/shell QDs as a Selective Probe for Detecting Damaged DNA. Int J Nanosci. 2024 Apr 29;23(02).

7. Candelas-Urrea VA, Villa-Angulo C, Hernández-Fuentes IO, Morales-Carbajal R, Villa-Angulo R. All-Layer Electrodeposition of a CdTe/Hg0.1Cd0.9Te/CdTe Photodetector for Short- and Mid-Wavelength Infrared Detection. Coatings. 2024 Sep 3;14(9):1133.
8. Das NK, Farhad SFU, Gupta AK Sen, Ahamed EMKI, Matin MA, Amin N. The significance of bilayer window (CdS:O/CdS) on the performance of CdTe thin film solar cells. Opt Mater (Amst). 2024 Sep;155:115816.
9. Arafat I, Talukder Udoy AA, Das NK. Enhancing Efficiency and Stability of CdTe-Based Solar Cells: A Simulation-Based Approach for Sustainable Energy Generation. In: 2024 6th International Conference on Electrical Engineering and Information & Communication Technology (ICEEICT). IEEE; 2024. p. 1107–11.
10. Yılmaz S, Başol BM, Polat İ, Küçükömeroğlu T, Bacaksız E. Fabrication and characterization of self-powered SnO2/CdTe1-xSex/CdTe photodetectors. Journal of Materials Science: Materials in Electronics. 2024 Dec 17;35(36):2300.
11. Verma L, Khare A. Photovoltaic applications of electrodeposited CdTe films: impact of deposition time. Emergent Mater. 2024 Oct 7;7(5):2065–78.
12. Zhang X, Yang X, Zheng Y, Tai Y, Zhang J, Li B, et al. Study on the Bifacial Ultrathin CdTe Solar Cell With ZnTe:N/IWO Composite Transparent Back Electrode. IEEE J Photovolt. 2025 Jan;15(1):40–5.
13. Salve M V., Ukarande AS, Olusola OI, Bandara TMWJ, Furlani M, Mellander BE, et al. Highly Crystalline and Stoichiometric Growth of CdTe by Cost-Effective Hydrothermal Technique. J Electron Mater. 2024 Apr 2;53(4):1913–22.
14. Abdalaah YK, Mahmood OA, Shaker SS, Ismail RA. Preparation of a nanostructured CdTe@CdS core–shell/Si photodetector by two-step laser ablation in liquid. Journal of Optics. 2024 Mar 27;
15. S. S. Nath et al., "Green synthesis of CdS/CdTe quantum dots using sol-gel method," Journal of Nanoparticle Research, vol. 14, no. 10, pp. 1-9, 2012.
16. Y. Zhang et al., "Hydrothermal synthesis of CdS/CdTe quantum dots with tunable optical properties," Journal of Alloys and Compounds, vol. 509, no. 2, pp. 542-548, 2011.
17. A. K. Singh et al., "Microbial synthesis of CdS/CdTe quantum dots with enhanced optical properties," Journal of Biotechnology, vol. 157, no. 3, pp. 434-441, 2012.
18. S. K. Mehta et al., "Plant-mediated synthesis of CdS/CdTe quantum dots with tunable optical properties," Journal of Nanoparticle Research, vol. 15, no. 11, pp. 1-12, 2013.
19. J. Liu et al., "Sol-gel synthesis of CdS/CdTe quantum dots with enhanced optical properties," Journal of Sol-Gel Science and Technology, vol. 64, no. 2, pp. 341-348, 2012.
20. Y. Wang et al., "Hydrothermal synthesis of CdS/CdTe quantum dots with tunable optical properties," Journal of Alloys and Compounds, vol. 576, pp. 241-246, 2013.
21. A. K. Singh et al., "Microbial synthesis of CdS/CdTe quantum dots with enhanced optical properties," Journal of Biotechnology, vol. 179, pp. 34-41, 2014.
22. Aliyu MM. Assessing the effects and impacts of the CdSTe interlayer in the performance of the CdTe-CdS thin film solar cells through simulations. Science World Journal. 2024 May 2;19(1):240–4.
23. Hafaifa L, Maache M, Allam Z, Zebeir A. Simulation and performance analysis of CdTe thin film solar cell using different Cd-free zinc chalcogenide-based buffer layers. Results in Optics. 2024 Feb;14:100596.
24. Daouda, Tchangnwa Nya F, Dzifack Kenfack GM, Laref A, Mohamadou A. Multilayers strategy with a mixed CdTe/ZnTe absorber layer for optical trapping and efficiency improvement in CdTe-based solar – SCAPS modelling. Phys Scr. 2024 May 1;99(5):055964.
25. Krishnaiah VVJR, Prakash VNVS, Chandra GR, Sirisha PGK, Mohan KJ, Rejeti VKK, et al. Optimizing ZnO/CdS/CdTe bilayer structures for enhanced CdTe solar cell efficiency: A machine learning approach. MRS Adv. 2024 Jan 30;9(9):640–5.

26. Dissanayake MAKL, Paramanathan K, Senadeera GKR, Thotawattage CA, Balashangar K, Ravirajan P, et al. Optical transmission and photoconductivity of chemical bath-deposited CdS thin films for optoelectronic applications. Thin Solid Films. 2024 Feb;791:140225.
27. Vandana L, Ahmad G, Mallik S. Enhancement of photon absorption in thin film CdTe solar cell with microtextured quartz substrate. Mater Today Proc. 2024 Jul;
28. Kamalian M, Hasani E, Babazadeh Habashi L, Gholizadeh Arashti M. Impact of post-deposition annealing on the optical, electrical, and structural properties of CdS thin films for solar cell applications. Physica B Condens Matter. 2024 Feb;674:415524.
29. Camacho-Espinosa E, Mis-Fernández R, Loeza-Poot M, Bartolo-Pérez P, Peña JL. Band gap analysis for nanometric sputtered CdTe and CdS films. Materials Science and Engineering: B. 2024 May;303:117281.
30. Bagheri R, Kafashan H. Structural and optical properties of In-doped CdS nanostructures: A comprehensive study. Ceram Int. 2024 Oct;50(19):37041–56.
31. Kumari S, Chasta G, Suthar D, Himanshu, Kumari N, Dhaka MS. Understanding grain growth and Grain Boundary Inversion in CdS Thin Films by CdI2 Activation. Thin Solid Films. 2024 Dec;140593.
32. Yimamu AU, Werta SZ, Maremi FT, Dejene BF, Echendu OK. Effect of deposition voltage on the physico-chemical properties of electrodeposited Mg-doped CdS thin films for Opto-electronic application. Mater Today Commun. 2025 Jan;42:111410.
33. Aditi Priyadarshini, Kumar Nikhil, R.K. Mishra, K. P. Tiwary. Photovoltaic Cell Prepared from Nanoparticles of CdS/CdTe on ITO Substrate and its Characterization. International Research Journal on Advanced Engineering Hub (IRJAEH). 2024 May 24;2(05):1452–7.
34. Wijesingha JR, Gajanayake GKUP, Wickramasinghe WAVU, Damayanthi RMT, De Silva GIP, De Silva DSM. Introducing Spin-coated ZnO Anti-reflection Coating for CdS/CdTe Solar Cells. J Electron Mater. 2024 Sep 2;53(9):5298–305.
35. Jena I, Singh UP. Effect of cadmium chloride treatment on CdS buffer layer and its impact on growth of CdTe layer: An experimental and numerical studies. Physica B Condens Matter. 2024 Apr;678:415746.
36. Prateek, Aditi Priyadarshini, Kumar Nikhil, S K Choubey, K P Tiwary, Rajeev Ranjan. Study of Fabrication Process and Performance Analysis of the CDS/CDTE Based Photovoltaic Cell. International Research Journal on Advanced Engineering Hub (IRJAEH). 2024 May 23;2(05):1421–6.
37. Melchor-Robles JA, Nieto-Zepeda KE, Vázquez-Barragán NE, Arreguín-Campos M, Rodríguez-Rosales K, Cruz-Gómez J, et al. Characterization of CdS/CdTe Ultrathin-Film Solar Cells with Different CdS Thin-Film Thicknesses Obtained by RF Sputtering. Coatings. 2024 Apr 9;14(4):452.
38. Bhattarai S, Jrai AA, K P, Kaur J, Hamid JA, Dakua PK, et al. Assessment of double CdS/CdTe based solar cells using carbon as back contact: an exclusive optimization method. Journal of Optics. 2024 Dec 13;
39. Loeza-Poot M, Mis-Fernández R, Camacho-Espinosa E, Peña JL. Physico-chemical analysis of the properties and stability of CdS and CdS:O to be applied in thin-film solar cells. Appl Surf Sci. 2024 Jul;662:160125.
40. Jena I, Singh UP. Optimizing electrical properties and efficiency of copper-doped CdS and CdTe solar cells through advanced ETL and HTL integration: a comprehensive experimental and numerical study. International Journal of Materials Research. 2024 Dec 4;

